



# Electrodeposition of copper from triethanolamine as a complexing agent in alkaline solution

Carolina Ramírez<sup>1</sup>, Benedetto Bozzini<sup>2</sup>, Jorge A. Calderón<sup>3,\*</sup>

<sup>1</sup> Grupo de Química Básica, Aplicada y Ambiente, Departamento de Ciencias Básicas, Instituto Tecnológico Metropolitano, Medellín, Colombia

<sup>2</sup> Department of Energy, Politecnico di Milano, via Lambruschini 4, 20156 Milano, Italy

<sup>3</sup> Centro de Investigación, Innovación y Desarrollo de Materiales – CIDEMAT, Universidad de Antioquia – UdeA, Calle 70 No. 52-21, Medellín, Colombia

## ARTICLE INFO

### Keywords:

Copper electrodeposition  
Non-cyanide bath  
Triethanolamine  
EQCM  
SERS  
Nucleation mechanism

## ABSTRACT

The use of triethanolamine (TEA) as a cyanide-free electrolyte for copper electrodeposition was studied. The effect of TEA concentration on electrodeposition rate and cathodic adsorption during 3D copper growth was investigated. Linear sweep voltammetry (LSV), electrochemical quartz crystal microbalance (EQCM), scanning electron microscope (SEM), chronoamperometry and in situ surface-enhanced Raman scattering (SERS) were used to achieve a kinetic, thermodynamic, and mechanistic understanding. TEA forms stable complexes with copper, the most stable being  $\text{Cu}(\text{TEA})(\text{OH})_3^-$ . Also, it acts as a surface modifier, promoting instantaneous nucleation and lower reduction rates to metallic copper. Thus, three-dimensional growth is controlled and, consequently, a smooth and homogeneous copper deposit is achieved.

## 1. Introduction

Copper is one of the most commonly electroplated metals and is used for numerous decorative and engineering applications [1]. Copper electrodeposits have been widely used in the electronic industry due to their high electrical conductivity. Furthermore, copper films have widespread application as a sublayer for other metal finishes, since they are capable of covering small imperfection of the substrate. Copper electrodeposition is achieved with two types of complex systems: acid (fluoroborate and sulphate solutions) and alkaline (cyanide and cyanide-free solutions). Acid electrolytes for copper electrodeposition is highly used in electroforming, metal finishing due to more current density can be applied in those solution, the current efficiency is high however its throwing power is poor, and it is not possible to apply this electrolyte directly onto active metals such zinc and steel [2]. Alkaline electrolytes for copper deposits are used as an undercoat deposit for other metals coatings in order to protect the substrate and improve the adhesion, the deposit produced for cyanide coatings are generally  $<12.5 \mu\text{m}$  [1]. Alkaline copper solutions have higher throwing power than other electrolytes. Alkaline baths are especially important for the industrial plating of steel and other substrates that can be prone to displacement reactions. Notwithstanding obvious toxicity and waste-treatment issues, cyanide complexes have been, and in practice

still are, the main constituents of alkaline aqueous electrolytes for copper electroplating. Non-cyanide alkaline electrolytes have been developed, using complexing agents such sorbitol [3], glycine [4], glycerol [5], glutamate [6] and pyrophosphate [7], that are safer and more environmentally-friendly. However, most of these electrolytes have shown serious practical limitations, such as high operating costs, low efficiency, and sensitivity to impurities. These limitations have hindered the implementation of cyanide-free electrolytes at industrial scale.

The nucleation mechanism for alkaline electrolytes have been less studied compared with acid electrolytes, however some studies have reported the nucleation mechanism based on Scharifker and Hills model, which describe the 3D grow mechanism in instantaneous or progressive nucleation [8]. The nucleation mechanism and electrocrystallization process depends on the electrolyte composition and the applied potential. Pesic et al. studied the mechanism of copper deposition in ammoniacal solutions at pH 8 where non uniform size particle distribution and progressive nucleation were found [9]. The same mechanism were reported in a electrolyte based on glycine at pH 10 [4]. Meanwhile smooth surface and instantaneous nucleation were found in electrolytes based on glutamate [6] and pyrophosphate [10] with sorbitol as additive. Recently, Lin et al. investigated the influence of some alcohols on copper electrodeposition from pyrophosphate-based electrolyte [11]. They conclude that all the coatings obtained under the influence of different

\* Corresponding author.

E-mail address: [andres.calderon@udea.edu.co](mailto:andres.calderon@udea.edu.co) (J.A. Calderón).

additives are pure copper, but glucose has advantage in reducing the grain size of copper coatings compared with other alcohols. Similarly, all the baths have the same electrocrystallization behavior, i.e., the irreversible and instantaneous nucleation process with 3D growth of nuclei controlled by the diffusion of  $[\text{Cu}(\text{P}_2\text{O}_7)_2]^{6-}$  specie.

TEA has been explored as a complexing agent for electrodeposition of Cu-Zn [12,13] in alkaline solution, and has been shown to be a versatile ligand even to obtain  $\text{CuInSe}_2$  and  $\text{CuAlGaSe}_2$  thin films [14,15]. Moreover, TEA is a non-toxic compound and is widely commercially available. In copper electrodeposition, Muralidharan et al. [16] have reported the use of TEA as an additive in citrate-based alkaline electrolytes, where it was shown to have a tendency to form more stable complexes than with citrate. Moreover, Liang et al. [17] used TEA as a second ligand added to 1-hydroxyethylene-1, 1-diphosphonic acid (HEDPA), and observed that an excess of TEA results in cathodic adsorption, promoting the formation of dense and homogeneous copper coatings. Notwithstanding its appeal, literature about the use of TEA for copper plating is scarce. Moreover, the TEA molecule has been used in conjunction with other additives and its individual contribution is hard to assess. Furthermore, a systematic study of the effect of TEA concentration on kinetics of copper deposition for the plating process is currently missing from the literature. Finally, direct molecular-level study of the adsorption behavior of this additive during the plating process has never been carried out.

With the aim of proposing a complexing agent as an alternative to cyanide electrolyte for copper electrodeposition, this work presents a systematic study of the use of TEA as the sole complexing agent of copper in an alkaline aqueous electrolyte, addressing the kinetics and adsorption processes. Specifically, the effects of TEA concentration on electrodeposition rate and on cathodic adsorption during 3D copper growth are investigated. In order to achieve a more insightful mechanistic understanding, electrochemical quartz crystal microbalance (EQCM) and *in situ* surface-enhanced Raman scattering (SERS) were used in addition to classical techniques. The former method allows the measurement of slight mass changes resulting from the electrochemical process and provides observables that can help elucidate the number and nature of electrodeposition steps [18]. Meanwhile, *In situ* SERS is particularly sensitive to Cu surfaces with nanometer-scale roughness [19], and can provide direct information on the dynamics and potential-dependent adsorption of organic molecules on the electrode.

## 2. Experimental

A three-electrode cell was used in the electrochemical studies. A rotating gold disk electrode (RDE) (Metrohm AG CH-9110 Herisau) and a gold disk were used as working electrodes. The counter electrode was a platinum mesh, and the reference electrode was Ag/AgCl 3 mol  $\text{L}^{-1}$  KCl. Before each deposition, the working electrode was polished with  $\text{Al}_2\text{O}_3$  powder (1  $\mu\text{m}$ ), cleaned ultrasonically with ethanol for 5 minutes, and finally washed with Milli-Q (12.8 M $\Omega$  cm) water.

The electrochemical measurements were carried out with a Gamry Instrument - reference 600 Potentiostat /Galvanostat. The electrolyte composition was 1.0 mol  $\text{L}^{-1}$  NaOH, 0.05 mol  $\text{L}^{-1}$   $\text{CuSO}_4 \cdot 5\text{H}_2\text{O}$ , to which variable amounts of TEA were added. The rotation speed of the working electrode was kept constant at 625 rpm. Linear sweep voltammetry was performed at a scan rate of 10  $\text{mV} \cdot \text{s}^{-1}$ . For potentiostatic transient experiments, the gold electrode disk was polished to a mirror finish with 0.3  $\mu\text{m}$  alumina powder. SERS spectra were recorded using a LabRAM microprobe confocal system. A 10 $\times$  long working-distance objective was used, with the excitation line at 632.8 nm. The slit and pinhole were set at 200 and 400  $\mu\text{m}$ , respectively. SERS activity of the Au working electrode was achieved by means of electrochemical oxidation – reduction cycles (ORC). The ORC protocol consisted of performing cyclic voltammetry measurements (CV) from 0.2 V to 1.2 V, for 50 cycles, with a scan rate of 500  $\text{mV} \cdot \text{s}^{-1}$ , in the cell used for Raman spectroscopy, to form SERS- active metal with 1.0 mol  $\text{L}^{-1}$  NaOH and 0.05

mol  $\text{L}^{-1}$  TEA as the electrolyte. The other bath components were added after the ORC protocol. The measurements were carried out under potentiostatic conditions, waiting for steady state current. The acquisition time of SERS spectra was c.a. 300 s.

Measurements of mass variation during copper electrodeposition were performed using an electrochemical quartz crystal microbalance (EQCM) from Metrohm Autolab. EQCM experiments were carried out using a Teflon® cell with a quartz crystal with active area of 0.361  $\text{cm}^2$ , coated with an evaporated gold film as the working electrode (WE). The basic oscillation frequency was set at 6 MHz. Cyclic voltammetry measurements (CV) were performed at a scan rate of 10  $\text{mV} \cdot \text{s}^{-1}$ , with simultaneous recording of the quartz resonance frequency.

The morphology of the coatings was evaluated using a scanning electron microscope (SEM) JEOL JSM 6490 LV.

## 3. Results and discussion

### 3.1. Effect of TEA concentration on voltammetric behavior

Fig. 1 shows the effect of TEA concentration on the LSV behavior of a copper electrodeposition bath containing:  $\text{CuSO}_4 \cdot 5\text{H}_2\text{O}$  (0.05 mol  $\text{L}^{-1}$ ) and NaOH (1.0 mol  $\text{L}^{-1}$ ).

It can be observed that, at lower concentrations of TEA (0.05 and 0.1 mol  $\text{L}^{-1}$ ), the initial reduction potential is less negative than for systems with higher TEA concentration. Moreover, changes in TEA concentration cause some variations in the voltammetric features. With electrolytes containing 0.5 and 1 mol  $\text{L}^{-1}$  TEA, two reduction process can be observed, labeled as A, which reaches a small plateau at approximately -0.6 V, and B, which reaches this at approximately -0.80 V, where the current density increases due to massive copper electrodeposition occurring in this potential range. The nature of these cathodic peaks will be described more extensively in Section 3.2, on the basis of EQCM study.

Regarding the LSV curves shown in Fig. 1, it was observed that the onset potential tends to shift to more negative potential with increasing the TEA content, indicating that TEA molecule induces a cathodic polarization of copper electrodeposition process. This phenomenon has also been observed in copper electrodeposition from alkaline electrolyte with alcohols and organic additives [11]. From LSV it is also evident that, the higher the TEA concentration, the lower the cathodic current density of Cu deposition at a given potential. Similar effects of variations

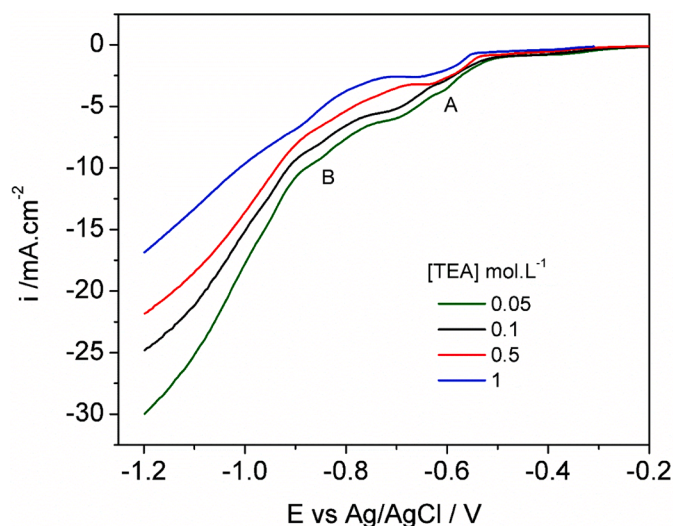


**Figure 1.** Linear sweep voltammograms for electrodeposition of copper at different TEA concentrations. Electrolyte: 1.0 mol  $\text{L}^{-1}$  NaOH, 0.05 mol  $\text{L}^{-1}$   $\text{CuSO}_4 \cdot 5\text{H}_2\text{O}$  and variable amounts of TEA. RDE was the working electrode at 625 rpm.

of TEA concentration on copper electrodeposition from HEDPA-containing alkaline baths were reported by Zheng et al. [17]. In that work, they explained the electrodeposition process with a “Coordination-Adsorption” theory, considering the two following phenomena:

- Cu(II) ions are more strongly complexed in the presence of a higher quantity of TEA. This means that the complexation decreases the activity of Cu(II) ions in solution, and consequently the reduction potential is shifted to more negative potentials.

- High quantities of TEA promote adsorption onto active sites of the electrode surface electrode, thus inhibiting the massive electrodeposition of copper.

The transport of the Cu-TEA complex by migration is hard due to its negative surface charge, so it is possible that some solvation of the complex specie must occur in order to facilitate its transport and the reduction of the Cu ions at the cathode. Although, as Cu-TEA complex is reduced at the cathode other transport phenomena like diffusion or convection will help to address the Cu ions to the electrode.

Thermodynamic computations were used to clarify the impact of Cu (II) complexing by TEA in alkaline environment, following the methodology described in [12], using the stability constants of the copper-TEA complexes from [20]. The computations were performed with the MEDUSA software [21]. The results of the thermodynamic analysis are reported in Fig. 2, which shows a diagram of the copper species distribution as a function of TEA concentration, at pH 14, with  $0.05 \text{ mol L}^{-1}$  of  $\text{Cu}^{2+}$  ions, and TEA concentrations in the range 0 to  $1.5 \text{ mol L}^{-1}$ . For TEA concentrations in excess of  $0.05 \text{ mol L}^{-1}$ , by far the most abundant complex formed is the ionic form  $[\text{Cu}(\text{TEA})(\text{OH})_3]^-$ . When the TEA concentration is less than  $0.1 \text{ mol L}^{-1}$ , the formation of copper oxide  $\text{CuO}(\text{s})$  precipitates is expected. Copper oxide formation at low TEA concentrations is due to the fact that, at high pH, the coordination sphere of Cu(II) consists mainly of  $\text{OH}^-$  ions, and this molecular arrangement promotes hydroxide/oxide formation, as a result of a condensation reaction [22]. Therefore, in order to obtain a stable electrolyte at pH 14, the Cu:TEA molar ratio should exceed 1:2. Excessive concentrations of TEA result in a reduction of the solubility of Cu(II), owing to the increase of the molar fraction of the  $\text{Cu}(\text{TEA})_2(\text{OH})_2$  complex, in which two TEA molecules complex each copper ion. Accordingly with Fig. 1, the onset potential tends to shift to more negative potential with higher concentrations of TEA. As is seen in Fig. 2, the difference in  $[\text{Cu}(\text{TEA})(\text{OH})_3]^-$  concentration is not

significant, in the same way, the cathodic shift is of the order of a few mV.

### 3.2. EQCM study of Cu electrodeposition from TEA electrolytes

The EQCM technique is used to record simultaneously electrochemical signal and changes in the resonance frequency  $\Delta f$  of a working electrode mounted on a piezoelectric oscillator, arising from mass-changes ( $\Delta m$ ) related to deposition, adsorption, or dissolution of species at the working electrode. The dependence of  $\Delta f$  on  $\Delta m$  is expressed through the Sauerbrey equation, Eq. (1):

$$\Delta f = -C_f \cdot \Delta m \quad (1)$$

Where  $\Delta f$  is measured in Hz,  $C_f$  is the sensitivity factor of the crystal ( $0.0815 \text{ Hz} \cdot \text{ng}^{-1} \cdot \text{cm}^{-2}$  for a 6 MHz at  $20^\circ\text{C}$ ) and  $\Delta m$  is given per unit area ( $\text{g} \cdot \text{cm}^{-2}$ ) [23].

In the case of electrodeposition, the correlation between changes in frequency and mass can be expressed in terms of charge, by combining the Faraday law and Sauerbrey equation, giving Eq. (2):

$$\Delta f = \frac{10^6 \cdot M_w \cdot C_f \cdot Q}{n \cdot F \cdot A_r} \quad (2)$$

Where:  $M_w$  is the apparent molar mass of the deposited metal ( $\text{g} \cdot \text{mol}^{-1}$ );  $Q$  is the integrated charge during electrodeposition (C);  $n$  is the number of electrons transferred during the discharge process;  $F$  is Faraday's constant ( $96485.33 \text{ C} \cdot \text{mol}^{-1}$ ) and  $A_r$  is the electrodeposition area of the working electrode.

EQCM experiments were carried out in order to characterize the cathodic current peaks A and B observed in Fig. 1, and to analyze the electrode reaction. The voltammograms and corresponding frequency variation traces  $\Delta f$  are presented in Fig. 3 for three different concentrations of TEA ( $0.1$ ,  $0.5$  and  $1 \text{ mol L}^{-1}$ ) in the electrolyte containing Cu (II)  $0.05 \text{ mol L}^{-1}$  and  $1 \text{ mol L}^{-1}$  NaOH. The CVs were recorded following the sequence: OCP  $\rightarrow -1.2\text{V} \rightarrow 0.3 \text{ V} \rightarrow$  OCP.

Notable differences were found in the positive scan between systems with high ( $0.5$  and  $1.0 \text{ mol L}^{-1}$ ) and low ( $0.1 \text{ mol L}^{-1}$ ) concentrations of TEA. In the systems with  $0.5$  and  $1.0 \text{ mol L}^{-1}$  of TEA the positive sweep is similar, and just one anodic peak, labeled C, was observed in the CV (Fig. 3b and 3c). On the other hand, in the electrolytes with  $0.1 \text{ mol L}^{-1}$  of TEA we observed two anodic peaks, labeled C and E. Additionally, a reactivation peak is present in the return scan, labeled F. Coherently

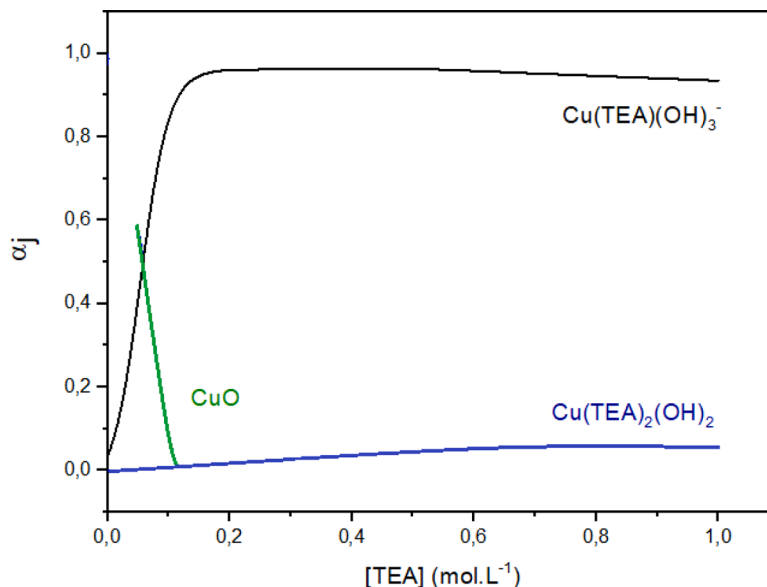


**Figure 2.** Distribution diagram of species stability. Molar fraction of copper species as a function of TEA concentration, computed as detailed in the text. Electrolyte:  $1.0 \text{ mol L}^{-1}$  NaOH,  $\text{mol L}^{-1}$   $\text{CuSO}_4 \cdot 5\text{H}_2\text{O}$   $0.05$  and TEA.

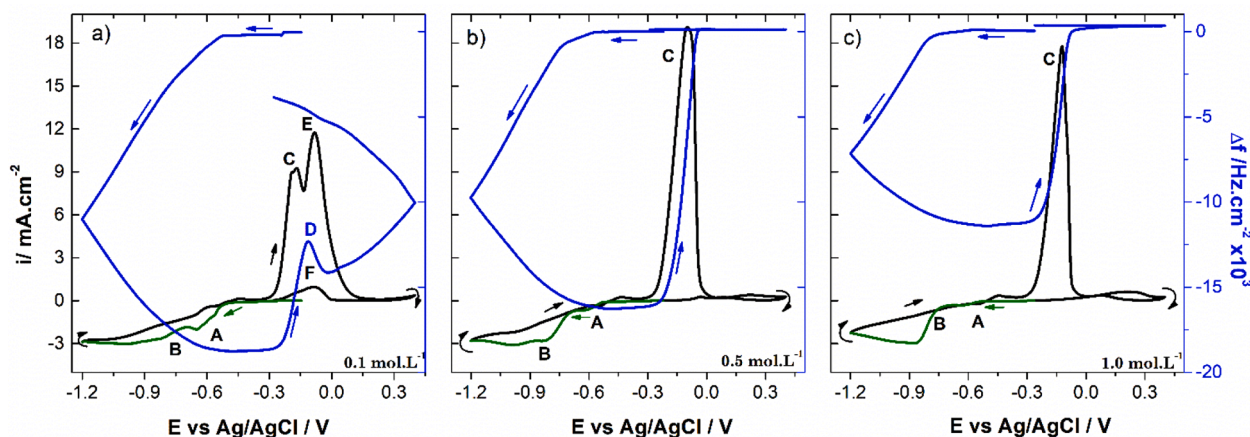
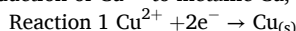


**Figure 3.** Cyclic voltammograms recorded simultaneously with  $\Delta f$  for electrolytes containing  $0.05 \text{ mol L}^{-1} \text{ Cu(II)}$ ,  $1 \text{ mol L}^{-1} \text{ NaOH}$  and different TEA concentrations in  $\text{mol L}^{-1}$ : a) 0.1 b) 0.5 c) 1.0.

with the LSVs reported in Fig. 1, the CVs show similar cathodic behavior, with two peaks (labeled A and B), and some differences in current intensity depending on TEA concentration.

In order to determine the nature of peaks A, B, C and E of Fig. 3, we evaluated the change of frequency  $\Delta f$  as a function of the circulated charge  $Q$ . From the linear relationship between  $\Delta f$  and  $Q$  stated by Eq. (2), it is possible to obtain the ratio  $M/z$ , where  $M$  is molar mass of the deposited species and  $z$  is the number of electrons transferred during the process. The ratio  $M/z$  allows mechanistic information to be derived regarding the electrochemical reactions prevailing in a given potential range. Table 1 reports the potential ranges where each peak appears in the CVs of Fig. 3 for the three concentrations of TEA studied. The results compiled in Fig. 3 and Table 1 confirm the linear relationship between  $\Delta f$  and  $Q$  in the potential range of peak A (around  $-0.5 \text{ V}$  to  $-0.7 \text{ V}$ ) for all three studied electrolytes. Specifically, a decrease of  $\Delta f$  is observed, indicating that an insoluble species is deposited on the electrode. Given that the reduction of  $\text{Cu(II)}$  to  $\text{Cu(I)}$  does not yield stable products, even in the presence of TEA [24], and the stoichiometric  $M/z$  value for 2-electron transference is  $31.7 \text{ g mol}^{-1}$ , the numerical results summarized in Table 1 suggest that peaks A and B (Fig. 3) are associated with the reduction of  $\text{Cu}^{2+}$  to metallic Cu, reaction 1:



According to EQCM results,  $\text{Cu(II)}$  ions are reduced directly to  $\text{Cu}_{(\text{s})}$  both in the simple-salt bath and in the presence of TEA complexes, regardless of the amount of TEA. The formation of an intermediate  $\text{Cu(I)}$  species may be possible. However, the half-life of this species is so short that it is practically not detected and it is not considered in the reaction mechanism. Similar reaction mechanism of copper electrodeposition has been reported in pyrophosphate baths with alcohols as additives, where  $[\text{Cu}(\text{P}_2\text{O}_7)_2]^{6-}$  was directly reduced to Cu, without formation of  $\text{Cu(I)}$

**Table 1**

$M/z$  values extracted from the slope of the resonator frequency change  $\Delta f$  versus circulated charge  $Q$  (Eq. (2)) for copper deposition and dissolution in electrolytes containing  $0.050 \text{ mol L}^{-1}$  of  $\text{Cu(II)}$ , different amounts of TEA (indicated in table) and  $\text{NaOH } 1.0 \text{ mol L}^{-1}$  ((c) – negative-going scan, (a) positive-going scan)

TEA concentration	Potential range (V)	Peak position	$M/z$ ( $\text{g mol}^{-1}$ )
$0.1 \text{ mol L}^{-1}$	-0.53 to -0.71	A (c)	$29.1 \pm 0.2$
	-0.67 to -1.20	B (c)	$28.11 \pm 0.02$
	-0.36 to -0.11	C (a)	$28.71 \pm 0.04$
	0.11 to 0.37	E (a)	$332 \pm 4$
$0.5 \text{ mol L}^{-1}$	-0.50 to -0.63	A (c)	$28.6 \pm 0.5$
	-0.63 to -1.20	B (c)	$29.59 \pm 0.02$
	-0.32 to 0.05	C (a)	$29.68 \pm 0.04$
$1.0 \text{ mol L}^{-1}$	-0.58 to -0.67	A (c)	$20.6 \pm 0.13$
	-0.67 to -1.20	B (c)	$27.22 \pm 0.01$
	-0.35 to 0.054	C (a)	$27.83 \pm 0.02$

specie [11]. Notwithstanding the similarity of the copper electrodeposition mechanism, discharge from aquo- and TEA-complexes impacts quantitative aspects of electrodeposition. Thus, a higher quantity of free  $\text{Cu(II)}$  ions is expected in electrolytes with low concentration of TEA. In fact, comparing the CV curves in Fig. 3, it can be observed that the intensity of peak A diminishes as TEA concentration increase. On the other hand, the intensity of peak B is accentuated in electrolytes with high TEA concentration. In the same way, the two slopes observed in the linear relationship between  $\Delta f$  and  $V$  in the potential ranges of peaks A and B are evidently associated with the different electrodeposition rates corresponding to peaks A and B, which in turn correlate with the relative amounts of the two different  $\text{Cu(II)}$  precursors. It can be inferred that the first cathodic peak A is due to copper discharge from the  $\text{Cu(II)}$  aquo-complex, while the cathodic peak B is associated with the reduction of the  $\text{Cu(II)-TEA}$  complex. Due to the presence of high concentrations of TEA, the complexes and TEA molecules are expected to adsorb on the electrode, blocking the active sites for reduction process of  $\text{Cu(II)}$  aquo-complex species. Therefore, the reduction of copper ions on the non-blocked sites is a slow process, as suggested by the low slope of the  $\Delta f$  vs.  $V$  curve in the potential range in the area of peak A. Then, at more negative overpotentials, massive copper reduction occurs (peak B), mainly from  $\text{Cu-TEA}$  complex, again obeying reaction 1. For obvious electrokinetic reasons, this last process is faster, as confirmed by the higher slope of the  $\Delta f$  vs.  $V$  curve in the potential range corresponding to peak B. Similar results have been reported for the reduction of copper ions in alkaline media in the presence of glycine as complexing agent [4].

Regarding the positive-going scan, peak C is in all cases related to the oxidation of metallic copper formed during the previous negative scan. In the experiments carried out with higher concentrations of TEA ( $0.5$  and  $1.0 \text{ mol L}^{-1}$ ), only one oxidation peak C is found. The voltammetric peak C precisely matches the progressive increase of  $\Delta f$ . This confirms that peak C is related with the dissolution of metallic copper formed in the foregoing negative scan to form  $\text{Cu(II)}$  in solution. In the electrolyte with lower TEA content ( $0.1 \text{ mol L}^{-1}$ ), the CV exhibits a double anodic peak (features C and E in Fig. 3a). Peak C begins at  $-0.3 \text{ V}$  and corresponds to  $\text{Cu(II)}$  formation, which is corroborated by  $\Delta f$  increase. At  $-0.17 \text{ V}$  the anodic current density starts to decrease and, correspondingly,  $\Delta f$  forms a peak, labeled as D, denoting an increase in the electrode mass. This oxidation reaction leads to a mass increase, confirmed by  $\Delta f$  decrease after peak D, which could be related to copper oxide formation and metal passivation: a well-known process for copper oxidation in alkaline media [25]. Moreover, the second oxidation peak (E) corresponds to the beginning of a progressive increase of  $\Delta f$ , indicating the start of the second active dissolution process concomitant with a decrease in the anodic current density due to diffusion limitation. This

behavior denotes weight loss of the working electrode, due to the dissolution of the previously oxide formed. It is worth noting that the  $M/z$  value measured for peak E ( $332 \text{ g}\cdot\text{mol}^{-1}$ ) cannot be correlated straightforwardly with the stoichiometry of the oxides formed in the positive scan. These discrepancies were discussed by Bertotti et al. [26] in terms of viscosity of the Cu(II) oxy-hydroxides forming in alkaline environment, leading to non-linearities in the dependence of  $\Delta f$  on  $Q$ . Similar considerations apply for the reactivation peak F, which is related to copper oxide dissolution during the reverse scan. No reactivation process (anodic peak F) was observed at high TEA concentration conditions.

The EQCM measurements show that copper oxide formation at anodic potentials can be avoided by using moderate concentrations of TEA in the electrolyte, higher than  $0.5 \text{ mol L}^{-1}$ . This effect is of great importance for industrial copper plating, because the efficiency of the process would be affected by the copper oxide formation if TEA concentration is below a critical level, while an appropriate amount of this additive promotes the complexation of Cu(II) ions, leading to active dissolution of the anode (avoiding electrode passivation) and effective bath replenishment.

With the aim of evaluating the plating bath efficiency and electro-deposition rate, the mass gain  $\Delta m$  at an electrical charge of  $-13 \text{ mC}$  in CV experiments at different TEA concentrations was evaluated using the data in Fig. 3. The values of the key electrodeposition parameters are reported in Table 2: (i)  $\Delta m$ ; (ii) the potential value  $E$  at which the target charge was reached and (iii) the cathodic efficiency.

From Table 2 it is evident that the higher the TEA concentration, the higher the potential needed to reach a charge of  $-13 \text{ mC}$ . Moreover, the quantity  $\Delta m$  of copper deposited on the electrode is inversely proportional to TEA concentration. These results show that the activity of Cu (II) decreases as a result of complexation with TEA, with a consequent decrease in the electrodeposition rate and the current efficiency. The reaction efficiency is not 100%, therefore a side reaction must consider. According to electrolyte composition the more probable side reaction that occur is the Hydrogen Evolution Reaction (HER). This scenario also suggests that TEA is adsorbed onto the cathode, thus diminishing the fraction of active sites available for electrodeposition. In order to gain direct evidence of the molecular composition of the electrochemical interface, we used *in situ* spectroelectrochemistry, as detailed in the next section.

### 3.3. SERS study of TEA behavior during copper electrodeposition

The cathodic behavior of TEA during copper electrodeposition has been studied by *in situ* SERS spectroscopy. In order to identify the specific influence of the presence of Cu ions on the interfacial behavior of TEA, TEA adsorption from Cu-free solutions at the bare gold working electrode was also studied. Figs. 4 and 5 summarize the key SERS results regarding TEA adsorption at the OCP (Fig. 4) and under cathodic polarization (Fig. 5) from  $1.0 \text{ mol L}^{-1}$  NaOH solutions with  $0.05 \text{ mol L}^{-1}$  TEA in the absence (Fig. 4, red plot) and the presence (Fig. 4, thick black plot and Fig. 5) of  $0.005 \text{ mol L}^{-1}$   $\text{CuSO}_4\cdot 5\text{H}_2\text{O}$ . At OCP, SERS spectra of TEA were measured both in the absence (red plot, OCP  $-423 \text{ mV}$ ) and in the presence (thick black plot, OCP  $-250 \text{ mV}$ ) of Cu(II) in solution (Fig. 4). In both electrolytes, a set of typical TEA bands is observed, matching the bulk TEA signals, with minor differences due to surface

**Table 2**

Electrodeposited mass after voltammetric circulation of  $-0.013 \text{ C}$  with three different concentrations of TEA. Data extracted from the CV and EQCM experiments of Fig. 3.

TEA concentration ( $\text{mol L}^{-1}$ )	E (V)	$\Delta m$ ( $\mu\text{g}$ )	Efficiency (%)
0.1	-0.75	$33.0 \pm 0.4$	77.10
0.5	-0.83	$30.1 \pm 0.6$	70.30
1.0	-0.90	$25.2 \pm 0.5$	58.87

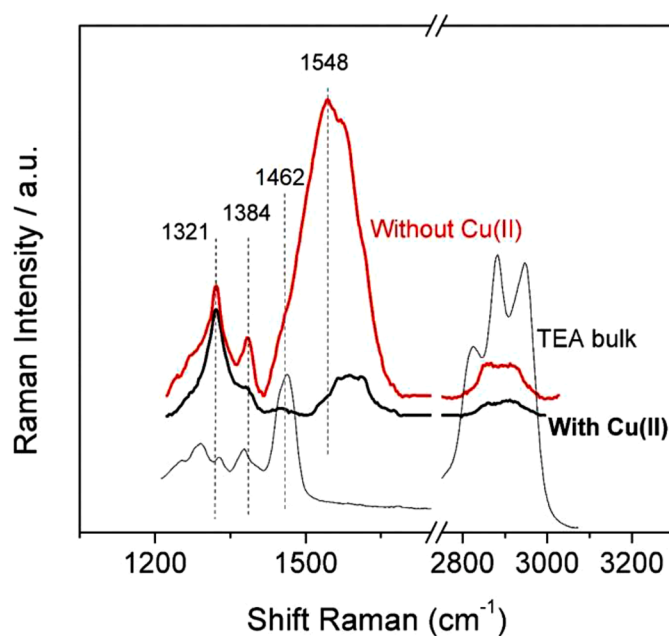


**Figure 4.** *In situ* SERS spectra measured on gold electrode at OCP ( $-250 \text{ mV}$ ). Electrolyte: NaOH  $1.0 \text{ mol L}^{-1}$ , TEA  $0.050 \text{ mol L}^{-1}$  without (red) and with (black)  $\text{CuSO}_4\cdot 5\text{H}_2\text{O}$   $0.005 \text{ mol L}^{-1}$ . Working electrode: Au. A normal Raman spectrum measured in the bulk of pure TEA is also shown for reference.

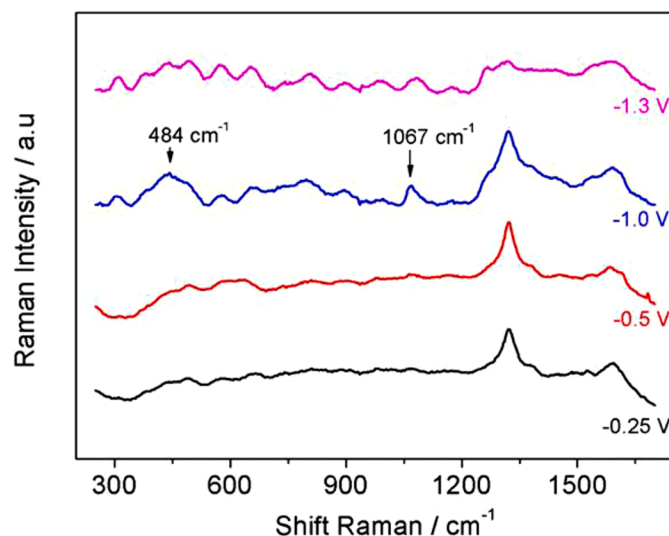


**Figure 5.** *In situ* Raman spectra measured at OCP ( $-250 \text{ mV}$ ) and different cathodic polarizations:  $-0.5$ ,  $1.0$  and  $-1.3 \text{ V}$ . Electrolyte:  $0.05 \text{ mol L}^{-1}$  TEA +  $1.0 \text{ mol L}^{-1}$  NaOH and  $0.005 \text{ mol L}^{-1}$   $\text{CuSO}_4\cdot 5\text{H}_2\text{O}$ . Working electrode: Au.

selection rules. These TEA characteristic bands are found at  $1321$ ,  $1384$ ,  $1462 \text{ cm}^{-1}$  and in the range  $2850\text{--}2930 \text{ cm}^{-1}$ . The assignment of these bands is given in Table 3. It is worth noting that the relative intensities of the TEA bands are different depending on the presence or absence of Cu (II) ions in the electrolytic bath, suggesting that the complexing of the cation has an impact on adsorption geometry. It is noted that the presence of Cu(II) ion inhibits the bands at  $1384$  and  $1462 \text{ cm}^{-1}$ , which are characteristic of  $\sigma\text{--CH}$  vibrational mode. Thus, according to the selection rules for SERS, it is possible to assume that C-H bonds are parallel to the surface electrode.

In addition to the TEA bands, we found other bands at ca.  $1548$  and  $1579 \text{ cm}^{-1}$ , the latter dominating in the presence of Cu(II). These new bands correspond to  $\text{CO}_2$  asymmetric stretching of a carboxylate group

**Table 3**

Assignment of Raman bands ( $\text{cm}^{-1}$ ) measured *in situ* during Cu electrodeposition and with bulk TEA, for reference.

In situ experiment / $\text{cm}^{-1}$	Measured bulk TEA and ref. [20] / $\text{cm}^{-1}$	Assignment of vibrational mode
308	309	vs (Cu-O)
484	481	vas (Cu-N)
575		Au-OH
792	796	$\sigma$ CH
1067	1066	$\nu$ OC
1321	1325	$\sigma$ CH + $\sigma$ OH
1384		$\sigma$ CH
1462	1468	$\sigma$ CH
1548		COOH
1579	1586	COOH
Broad band	2825	$\nu$ CH
2850-2930	2878	$\nu$ CH
	2948	$\nu$ CH

bonded to a metal atom [27]. Moreover, it can be observed that, in the presence of Cu(II) ions in the electrolyte, the bands in the 1548-1579  $\text{cm}^{-1}$  range decrease in intensity. This suggests that the electrode surface coverage with carboxylate compounds is smaller in the presence of Cu (II) ions. These results concerning carboxylate formation during ORC are coherent with previous works [19,20], which reported that TEA tends to react under anodic polarization, producing nitrilotriacetic acid. Alcoholamines are in fact known to form coordination complexes with the surface of the electrode by sharing the electron lone pairs of nitrogen or oxygen with the metal electrode [28]. The carboxylates produced anodically can form soluble complexes with copper ions. In this way, in the absence of Cu ions, carboxylates are directly attached to the metal surface [29], while when the electrolyte contains Cu ions, the corresponding complex tends to adsorb weakly. It is worth noting that the electrochemical behavior of TEA also depends on the kind of metallic cation present in the electrolyte. Indeed, in a previous work [30] it was shown that, under similar conditions for Cu and Zn electrodeposition, the SERS spectra of TEA were not appreciably modified in the presence or absence of Zn ions in the electrolyte. This can be straightforwardly explained by the fact that TEA and Zn(II) do not form stable complexes.

In order to obtain surface chemical information during copper electrodeposition, *in situ* Raman spectra were taken in the steady state conditions reached after 300 s of potentiostatic cathodic polarization at four representative potentials. The key results are shown in Fig. 5, highlighting the Raman shift interval in which evident changes in spectral pattern appear when changing the potential. It can be observed that, at cathodic potentials up to -1.0 V, the dominant band is the adsorbed TEA band at 1321  $\text{cm}^{-1}$  related with the CH - OH vibration representative of OCP (-0.25 V) conditions, while this tends to disappear at higher cathodic polarizations. When -1.0V is applied, other weaker TEA bands appear at 1067  $\text{cm}^{-1}$ , 792  $\text{cm}^{-1}$ , and 484  $\text{cm}^{-1}$ , related to O-C stretching, C-H stretching and Cu-N stretching, respectively. At this potential the electrode surface is covered by copper, the described interaction is now between Cu surface and TEA molecule. Apart from the presence of the band at 1321  $\text{cm}^{-1}$ , the spectral scenario under cathodic polarization is the same as that found by Ramírez et al. during Zn electrodeposition [30]. A similar interpretation in terms of a change of TEA adsorption geometry applies here. Briefly, at OCP and low cathodic potentials, TEA adsorption is dominated by metal-O bonding, while at higher cathodic potentials the metal-N bond takes over and eventually TEA desorbs at very high cathodic polarizations. In Fig. 6 a scheme of the Cu-TEA complex adsorption on the gold electrode during copper deposition is presented, based on SERS information.

### 3.4. Morphological study

In order to analyze the effect of TEA adsorption during copper electrodeposition, we performed SEM observations of two copper

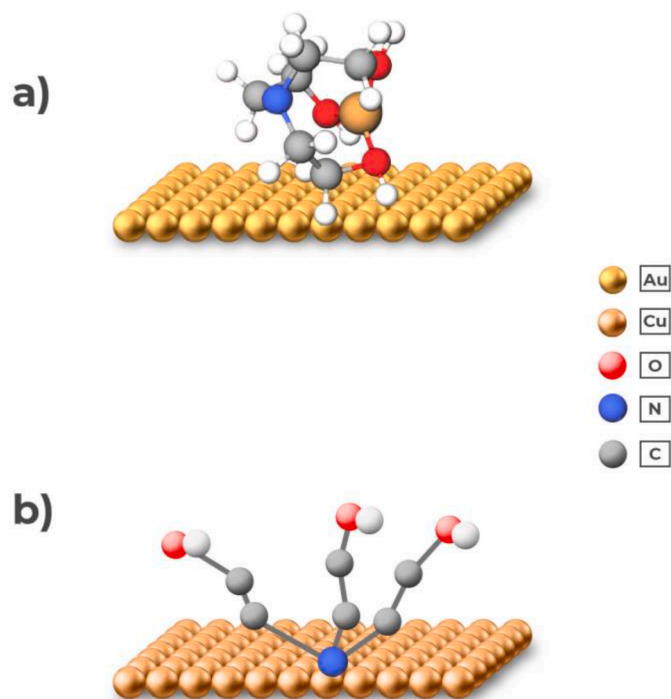


**Figure 6.** Scheme of Cu-TEA complex adsorption on gold electrode. (a) Low cathodic polarization, (b) high cathodic polarization (copper electrodeposition).

coatings obtained at different TEA concentrations in the electrolyte. The coatings were obtained by plating for 150 s at a potentiostatic cathodic polarization of -1.0V from electrolytes containing 0.1 and 1.0 mol  $\text{L}^{-1}$  TEA. The choice of -1.0V as the potential applied for electrodeposition is dictated by the fact that, at this potential polarization, massive copper reduction occurs (after peak B in Fig. 3) mainly from Cu-TEA complex. Fig. 7 shows the SEM images of the surface of the obtained electrodeposits.

The SEM micrographs show an evident effect of TEA concentration on the coating morphology. Fig. 7(a) shows that a low TEA concentration in the electrolyte correlates with a homogeneous, but defective morphology. This can be explained by the fact that low amounts of TEA are not effective in suppressing internal stress and dendritic growth of the copper coating. With higher concentrations of TEA, smooth and homogeneous copper deposits can be instead obtained. Coherently with EQCM experiments, the adsorption of TEA on the electrode surface diminishes the metal electrodeposition rate, leading to a less massive deposit and better atomic organization of the metallic copper. This behavior suggests that TEA also acts as a surface modifier, promoting instantaneous nucleation as a consequence of the adsorption of TEA molecules simultaneously with copper reduction. This promotes an arrangement of the reduced copper into nanocrystallites, correlating with better functional and decorative properties.

In order to assess the role of TEA in the nucleation and growth kinetics of copper during electrodeposition, chronoamperometric transients were measured at -1.0 V, at different TEA concentrations, Figs. 8 and 9. The characteristic maximum in the transient curves is due to the nucleation and growth of copper nuclei [31]. Similarly, to the CV analysis in Fig. 3, the higher the TEA concentration, the lower the current density value of the maximum. From Fig. 8, it can also be observed that the time at which the maximum current value is reached tends to correlate with TEA concentration.

The data from Fig. 8 were replotted in dimensionless form in Fig. 9, together with the theoretical curves derived for instantaneous (Eq. (3)) and progressive (Eq. (4)) nucleation models [8] obtained from Eq.s 3 and 4.

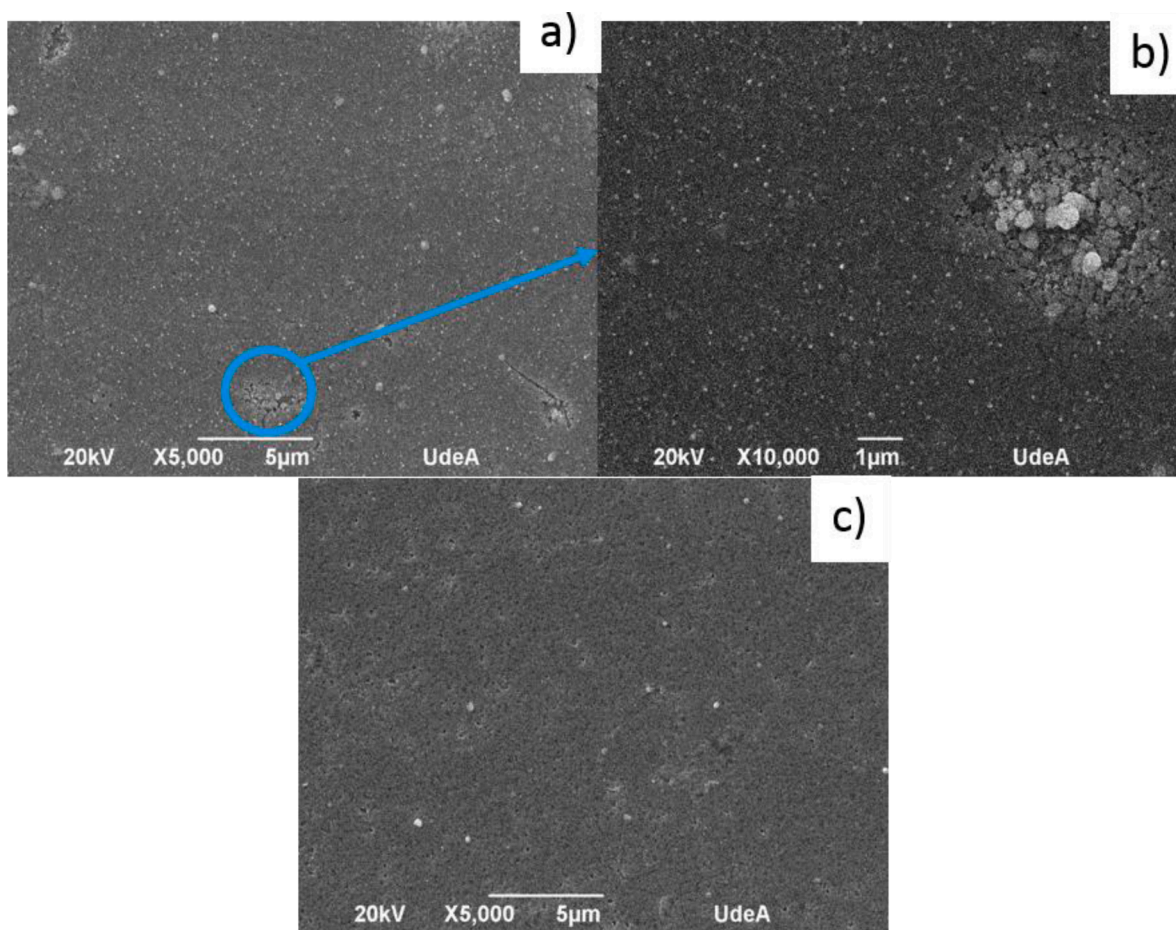


**Figure 7.** SEM micrographs of copper coatings obtained from an electrolyte composed of  $0.05 \text{ mol L}^{-1} \text{ CuSO}_4$ , and  $1 \text{ mol L}^{-1} \text{ NaOH}$  containing (a) and (b)  $0.1 \text{ mol L}^{-1} \text{ TEA}$ . (c)  $1.0 \text{ mol L}^{-1} \text{ TEA}$ . Potentiostatic deposition at  $-1.0 \text{ V}$  for  $150 \text{ s}$

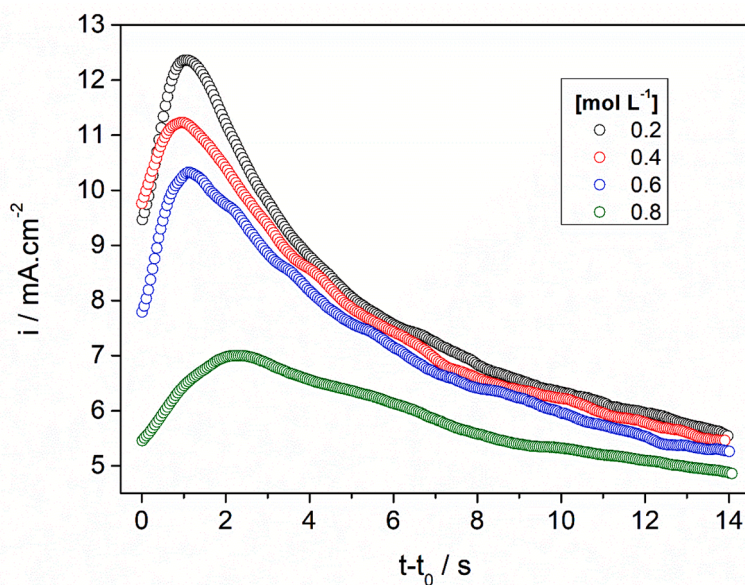


**Figure 8.** Chronoamperometric transients obtained applying a potentiostatic step of  $-1.0 \text{ V}$  to a gold cathode in contact with electrolytes with different concentrations of TEA:  $0.2, 0.4, 0.6$  and  $0.8 \text{ mol L}^{-1}$

$$(i_{inst}/i_{max})^2 = 1.9542(t/t_{max})^{-1} \{1 - \exp[-1.2564 (t/t_{max})]\}^2 \quad (3)$$

$$(i_{prog}/i_{max})^2 = 1.2254(t/t_{max})^{-1} \{1 - \exp[-2.3367 (t/t_{max})^2]\}^2 \quad (4)$$

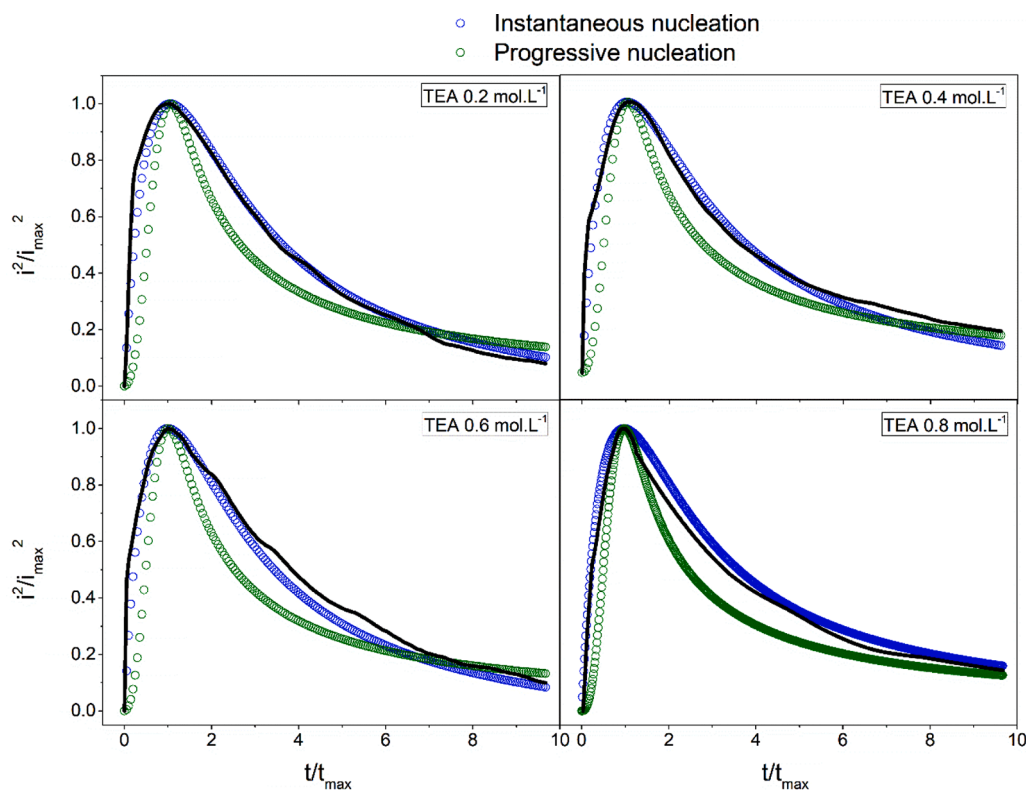


**Figure 9.** Comparison between dimensionless theoretical and experimental current transient curves, obtained at -1.0V at the different TEA concentration. The theoretical curves refer to instantaneous (blue) and progressive (green) nucleation.

Good coherence can be observed between the instantaneous nucleation mechanism for the first nucleation states and the different TEA concentrations considered. This result suggests that the copper nuclei are formed rapidly at the beginning of the electrodeposition and, once formed, grow until merging with neighbor nuclei. Instantaneous nucleation can promote uniform coatings, given that all nuclei can grow at the same time and at the same velocity. Accordingly, these results are consistent with the SEM images observed in Fig. 7, where the presence of TEA promotes uniform copper coatings, inhibiting dendritic growth. However, at low TEA concentration, like  $0.1 \text{ mol L}^{-1}$  or less, the kinetics of copper electrodeposition is fast (CV of Fig. 3) promoting some defects of the coating, as can be seen in the Fig. 7a, b. In those conditions the correlation between nucleation mechanism and macroscopic behaviors is still valid, and the nucleation mechanism could change from instantaneous to progressive. However, the nucleation mechanism was not evaluated at that low TEA concentrations.

Similar results were obtained for copper electrodeposition in an alkaline electrolyte using different alcohols as additives [10,11]. According to the authors, the hydroxyl groups adsorbed on the cathode alter the double layer structure, since the molecular nature of the additive can influence the adsorption energy on the electrode. Considering different alcohols, the higher the molecular weight, the lower the adsorption energy, which in turn affects the particle size [7].

#### 4. Conclusions

This work proposed an electrolyte based on TEA to electrodeposit copper from a cyanide-free alkaline electrolyte. The electrochemical behavior of the system depends on the concentration of TEA in the electrolyte. At low TEA concentrations,  $\text{Cu}_2\text{O}$  can form in the electrolyte, yielding suboptimal deposits and poor performance of soluble anodes. However, with a relatively high concentration of TEA, the most stable complex is  $\text{Cu}(\text{TEA})(\text{OH})_3$ , which is reduced directly to Cu.

*In situ* SERS was used to study the electrode-electrolyte interface at

molecular level. In the absence of Cu(II) ions, higher surface coverages with TEA are found, since Cu(II)-TEA complexes tend to adsorb less than free TEA. On increasing the cathodic potential, adsorbed TEA undergoes a reorientation from mainly O-bonded to N-bonded, and eventually desorbs at high polarizations.

The effect of TEA on the investigated electrolyte is to form the stable complexes  $\text{Cu}(\text{TEA})(\text{OH})_3$ ; moreover, it also acts as a surface modifier, promoting instantaneous nucleation and lower reduction rates to metallic copper. Thus, the three-dimensional growth is controlled, and consequently smooth and homogeneous copper deposit is achieved.

#### CRediT authorship contribution statement

**Carolina Ramírez:** Investigation, Validation, Writing – original draft. **Benedetto Bozzini:** Methodology, Data curation, Writing – original draft. **Jorge A. Calderón:** Conceptualization, Methodology, Funding acquisition, Writing – review & editing.

#### Declaration of Competing Interest

The authors declare that they have no known competing financial interests or personal relationships that could have appeared to influence the work reported in this paper.

#### Data availability statement

Data available on request from the interested.

#### Acknowledgments

The authors would like to thank the Universidad de Antioquia for the financial support given for this work through the “Estrategia de Sostenibilidad” and the 2015-8323 project. Carolina Ramírez wishes to thank



Colombian Ministry of Science, Technology, and Innovation “Min-ciencias” for her doctoral scholarship grant and ENLAZAMUNDOS for their financial support of the internship in Università del Salento (Italy). The authors also thank the electrochemical laboratory of the Università del Salento, Lecce.

## References

- [1] M. Schlesinger, M. Puunovic, *Modern Electroplating*, 5th ed., John Wiley & Sons, New Jersey, 2010.
- [2] L. Fabbri, W. Giurlani, G. Mencherini, A. De luca, M. Passaponti, et al., Optimisation of thiourea concentration in a decorative copper plating acid bath based on methanesulfonic electrolyte, *Coatings* 12 (2022) 376, <https://doi.org/10.3390/coatings12030376> [Online]. Available:.
- [3] Z.A. Hamid, a.A. Aal, New environmentally friendly noncyanide alkaline electrolyte for copper electroplating, *Surf. Coatings Technol.* 203 (10–11) (2009) 1360–1365, <https://doi.org/10.1016/j.surfcoat.2008.11.001>. Feb.
- [4] J.C. Ballesteros, E. Chainet, P. Ozil, G. Trejo, Y. Meas, Initial stages of the electrocrystallization of copper from non-cyanide alkaline bath containing glycine, *J. Electroanal. Chem.* 645 (2) (2010) 94–102, <https://doi.org/10.1016/j.jelechem.2010.05.002>. Jul.
- [5] P. Sivasakthi, R. Sekar, G.N.K. Ramesh Babu, Electrodeposition and characterisation of copper deposited from cyanide-free alkaline glycerol complex bath, *Trans. IMF* 93 (2015) 32–37, <https://doi.org/10.1179/1743294414Y.0000000400>.
- [6] P. Pary, L.N. Bengoa, W.A. Egli, Electrochemical characterization of a Cu(II)-glutamate alkaline solution for copper electrodeposition, *J. Electrochem. Soc.* 162 (7) (2015) D275–D282, <https://doi.org/10.1149/2.0811507jes>.
- [7] Q. Li, J. Hu, J. Zhang, P. Yang, Y. Hu, M. An, Screening of electroplating additive for improving throwing power of copper pyrophosphate bath via molecular dynamics simulation, *Chem. Phys. Lett.* 757 (2020), 137848, <https://doi.org/10.1016/j.cplett.2020.137848>. Oct.
- [8] B. Scharifker, G. Hills, Theoretical and experimental studies of multiple nucleation, *Electrochim. Acta* 28 (7) (1983) 879–889, [https://doi.org/10.1016/0013-4686\(83\)85163-9](https://doi.org/10.1016/0013-4686(83)85163-9).
- [9] D. Grujicic, B. Pesic, Reaction and nucleation mechanisms of copper electrodeposition from ammoniacal solutions on vitreous carbon, *Electrochim. Acta* 50 (22) (2005) 4426–4443, <https://doi.org/10.1016/j.electacta.2005.02.012>.
- [10] C. Lin, J. Hu, Q. Zhang, J. Zhang, et al., Deciphering the levelling mechanism of sorbitol for copper electrodeposition via electrochemical and computational chemistry study, *J. Electroanal. Chem.* 880 (2021), 114887, <https://doi.org/10.1016/j.jelechem.2020.114887>. Jan.
- [11] C. Lin, J. Hu, J. Zhang, Y. Peixia, X. Kong, A comparative investigation of the effects of some alcohols on copper electrodeposition from pyrophosphate bath, *Surf. Interfaces* 22 (2021), 100804.
- [12] C. Ramírez, J.A. Calderón, Study of the effect of Triethanolamine as a chelating agent in the simultaneous electrodeposition of copper and zinc from non-cyanide electrolytes, *J. Electroanal. Chem.* 765 (2015) 132–139, <https://doi.org/10.1016/j.jelechem.2015.06.003>.
- [13] S. Vivegnis, J. Delhalle, Z. Mekhalif, F.U. Renner, Copper–zinc alloy electrodeposition mediated by triethanolamine as a complexing additive and chemical dealloying, *Electrochim. Acta* 319 (2019) 400–409, <https://doi.org/10.1016/j.electacta.2019.07.007>.
- [14] P. Prabukanthan, et al., Influence of complexing agents-aided CuInSe<sub>2</sub> thin films by single-step electrochemical deposition and photoelectrochemical studies, *J. Mater. Sci. Mater. Electron.* 32 (6) (2021) 6855–6865, <https://doi.org/10.1007/s10854-021-05390-y>.
- [15] K. Rodríguez-Rosales, et al., One-step electrodeposition of CuAlGaSe<sub>2</sub> thin films using triethanolamine as a complexing agent, *Thin Solid Films* 713 (September) (2020), 138351, <https://doi.org/10.1016/j.tsf.2020.138351>.
- [16] C.L. Aravinda, S.M. Mayanna, V.S. Muralidharan, Electrochemical behaviour of alkaline copper complexes, *Proc. Indian Acad. Sci.* 112 (5) (2000) 543–550, <https://doi.org/10.1007/BF02709287>.
- [17] J. Zheng, H. Chen, W. Cai, J. Zhou, L. Qiao, L. Jiang, Mechanisms of triethanolamine on copper electrodeposition from 1-hydroxyethylene-1,1-diphosphonic acid electrolyte, *J. Electrochem. Soc.* 164 (12) (2017) D798–D801, <https://doi.org/10.1149/2.0091713jes>.
- [18] K. Mech, P. Zabiński, R. Kowalik, K. Fitzner, EQCM, SEC and voltammetric study of kinetics and mechanism of hexaamminecobalt(III) electro-reduction onto gold electrode, *Electrochim. Acta* 81 (2012) 254–259, <https://doi.org/10.1016/j.electacta.2012.07.067>.
- [19] M.E. Abdelsalam, P.N. Bartlett, J.J. Baumberg, S. Cintra, T.A. Kelf, A.E. Russell, Electrochemical SERS at a structured gold surface, *Electrochem. Commun.* 7 (7) (2005) 740–744, <https://doi.org/10.1016/j.elecom.2005.04.028>.
- [20] P. De Vreese, A. Skoczyla, E. Mattheijs, J. Franssaer, K. Binneemans, Electrodeposition of copper-zinc alloys from an ionic liquid-like choline acetate electrolyte, *Electrochim. Acta* (2013), <https://doi.org/10.1016/j.electacta.2013.06.140>. Jul.
- [21] I. Puigdomenech, *Hydra/Medusa Chemical Equilibrium Database and Plotting Software*, KTH Royal Institute of Technology, 2004.
- [22] J.-P. Jolivet, C. Chanéac, D. Chiche, S. Cassaignon, O. Durupthy, J. Hernandez, Basic concepts of the crystallization from aqueous solutions: The example of aluminum oxy(hydroxi)des and aluminosilicates, *C. R. Geosci.* 343 (2–3) (2011) 113–122, <https://doi.org/10.1016/j.crte.2010.12.006>.
- [23] G. Sauerbrey, Verwendung von Schwingquarzen zur Wägung dünner Schichten und zur Mikrowägung, *Z. für Phys.* 155 (2) (1959), <https://doi.org/10.1007/BF01337937>.
- [24] R.I. Drissi-Daoud A, A. Darchen, Electrochemical investigation of copper behaviour in different cupric complex solutions: voltammetric study, *J. Appl. Electrochem.* 33 (2003) 339–343.
- [25] J. Zheng, B. Zheng, Y. Ying, L. Qiao, L. Jiang, C. Zhang, Anodic behavior of copper in 1-hydroxyethylene-1,1-diphosphonic acid (HEDPA) baths, *Adv. Mater. Res.* 472–475 (2012) 3–7, <https://doi.org/10.4028/www.scientific.net/AMR.472-475.3>.
- [26] T.R.L.C. Paixão, E.A. Ponzio, R.M. Torresi, M. Bertotti, EQCM behavior of copper anodes in alkaline medium and characterization of the electrocatalysis of ethanol oxidation by Cu(III), *J. Braz. Chem. Soc.* 17 (2) (2006) 374–381, <https://doi.org/10.1590/S0103-50532006000200023>.
- [27] E.J. Salazar-Sandoval, M.K.G. Johansson, A. Ahnizay, Aminopolycarboxylic acids as a versatile tool to stabilize ceria nanoparticles – a fundamental model experimentally demonstrated, *RSC Adv.* 4 (18) (2014) 9048, <https://doi.org/10.1039/c3ra45875j>.
- [28] T. Łuczak, Electrochemical oxidation of alcoholamines at gold, *J. Appl. Electrochem.* 37 (6) (2007) 653–660, <https://doi.org/10.1007/s10800-007-9314-4>.
- [29] S. Karastogianni, S. Girousi, Electrochemical behavior of triethanolamine at a carbon paste electrode, *Sens. Electroanal.* 8 (2014) 241–252 [Online]. Available: <http://dspace.upce.cz/handle/10195/58401>.
- [30] C. Ramírez, B. Bozzini, J. Calderón, In situ SERS and ERS assessment of the effect of triethanolamine on zinc electrodeposition on a gold electrode, *Electrochim. Acta* 248 (2017) 270–280, <https://doi.org/10.1016/j.electacta.2017.07.095>.
- [31] D. Pletcher, G. R. R. Peat, L.M. Peter, J. Robinson, *Instrumental Methods in Electrochemistry*, Cambridge: Woodhead Publishing, 2002.